Articles

Modulation of the Redox Properties of the Flavin Cofactor through Hydrogen-Bonding Interactions with the N(5) Atom: Role of αSer254 in the Electron-Transfer Flavoprotein from the Methylotrophic Bacterium W3A1

Kun-Yun Yang[‡] and Richard P. Swenson*[,‡,§]

Biophysics Program and Department of Biochemistry, The Ohio State University, Columbus, Ohio 43210

Received August 10, 2006; Revised Manuscript Received December 19, 2006

ABSTRACT: The functional effects of hydrogen-bonding interactions at the N(5) atom of the flavin cofactors in the oxidized state have not been well established in flavoproteins. The unique properties of the electron-transfer flavoprotein from the methylotrophic bacteria W3A1 (wETF) were used to advantage in this study to evaluate this interaction. In wETF, the side-chain hydroxyl group of αSer254 serves as a hydrogen bond donor to the N(5) atom in the oxidized state of the flavin. The strength of this hydrogen bond was systematically altered by the substitution of αSer254 with threonine, cysteine, or alanine by site-directed mutagenesis. The anionic semiquinone form of the flavin, which is highly stabilized both thermodynamically and kinetically in the wild-type protein, was observed to accumulate in all three mutants. However, the midpoint potential for the first couple ($E_{ox/sq}$) was significantly decreased for all of the mutants, and the kinetic barrier toward the reduction of the anionic semiquinone that is observed in the wild-type wETF was effectively abolished in the αS254T and αS254C mutants. Based on the observed changes in the K_d values and associated binding energies for the flavin, the amino acid replacements destabilize both the oxidized and semiquinone states of the flavin, but to a much greater extent for the anionic semiquinone state. The $E_{ox/sq}$ values for the αSer254 mutants follow a general trend with the strength of N(5) H-bond in the oxidized state as indicated by Raman spectral analyses. These results support the conclusion that the H-bonding interaction at the N(5) plays a key role in establishing the high $E_{ox/sq}$ and the unusually high stability of the anionic semiquinone state in wETF.

Flavoproteins can efficiently participate in a wide variety of essential biochemical processes in both prokaryotic and eukaryotic cells including electron transfer, dehydrogenation, signal transduction, and various photobiological processes (*1*). The interactions between the flavin cofactor and its binding site on the apoprotein are critical for establishing the remarkable versatility of the cofactor in the biological functions of flavoproteins. The means by which these interactions modulate the physical and chemical properties of the flavin, including its midpoint potentials and the accessibility to specific redox states, have been studied extensively. Interactions that have been demonstrated to be important include hydrogen-bonding interactions at N(1) (*2*, *3*), N(3) (*4*), N(5) (*5*−*7*), and C(4)O (*8*, *9*), the short- and long-range electrostatic interactions (*6*, *10*−*12*), the $\pi-\pi$ stacking of the isoalloxazine ring with aromatic residues of the apoprotein (*11*, *13*, *14*), and donor atom−flavin interactions (*15*). The solvent accessibility of the isoalloxazine ring and the conformational factors of both the isoalloxazine ring and the local peptide backbone also play crucial roles (*1*, *7*, *16*). Most of these interactions have been systematically explored in our laboratory by using the *Desulfovibrio vulgaris* and *Clostridium beijerinckii* flavodoxins as very effective model systems (*4*, *5*, *7*, *10*−*12*, *14*−*16*).

Although these flavodoxins provide a unique set of properties, including the lowest midpoint potential observed for flavoproteins as well as the thermodynamic stabilization of neutral semiquinone (*17*), other interactions not found there require further study. For example, hydrogen-bonding interactions with the N(5) atom are absent in the oxidized state in these proteins (*18*), but have been studied in the reduced states in which the N(5)H serves as a hydrogen bond (H-bond) donor (*5*, *6*). Because of the essential role played by the N(5) position in the redox reactions and other chemical processes of the flavin, greater knowledge of the effects of hydrogen bonding at N(5) in all three redox states on the properties of the flavin is of importance (*19*, *20*).

Hydrogen-bonding interactions with the N(5) atom in the oxidized state of the flavin can be found in other flavoproteins such as in the old yellow enzyme from brewer's yeast

* To whom correspondence should be addressed. Tel: 614-292-9428. Fax: 614-292-6773. E-mail: swenson.1@osu.edu.

[‡] Biophysics Program.

[§] Department of Biochemistry.

10.1021/bi0616293 CCC: $37.00
Published on Web 02/10/2007

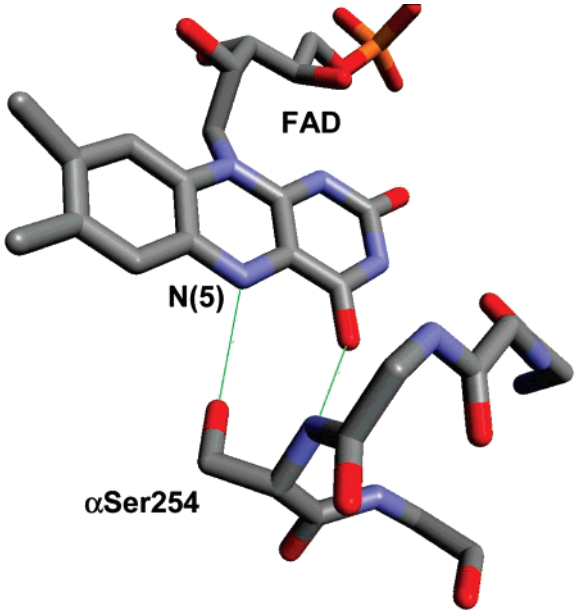

FIGURE 1: H-bonding interactions between the N(5) and C(4)O moieties of the FAD cofactor and the side-chain hydroxyl and main chain NH groups, respectively, of αSer254 in the wETF based on its crystal structure (PDB code, 1O97). Note that only a portion of the FAD cofactor and the main-chain atoms of the adjacent amino acid residues in this loop (-V-G-Q-$\mathbf{S}_{254}$-G-) are shown for greater clarity.

(*21*) and the flavin mononucleotide binding domain of flavocytochrome P450BM-3 from *Bacillus megaterium* (*22*). Unfortunately, in these cases, H-bonds are provided by peptide backbone amide groups within the apoprotein. This greatly complicates the analyses of these interactions using, for example, standard site-directed mutagenesis approaches. Attempts to eliminate the hydrogen-bonding interactions by reconstitution with the analogue 5-deazaflavin (*23*) or the substitution of the donor residue by proline, which lacks the amide hydrogen (*24*), have not been very fruitful.

The electron-transfer flavoprotein from the methylotrophic bacterium W3A1 (designated throughout as wETF)[1] (*25*, *26*) provides a good system for studying this aspect. In the oxidized (OX) state, the N(5) of the noncovalently bound flavin adenine dinucleotide (FAD) cofactor is hydrogen-bonded directly to the side-chain hydroxyl group of αSer254, which serves as the H-bond donor (Figure 1) (*27*). This protein also has several unique properties that are complementary to the flavodoxin, including the highest midpoint potential for the ox/sq couple thus far observed for flavoproteins, a highly stabilized anionic flavin semiquinone (SQ) state, and an unusual kinetic barrier to the formation of the hydroquinone (HQ) state (*28*). In addition, the wETF is a structural and functional homologue of the mammalian ETF, an essential flavoprotein in mitochondrial catabolism (*29*, *30*). The naturally occurred pathogenic mutations of human ETF are frequently found to involve αThr266 (*31*), the homologue of αSer254 in wETF, implying the important role played by αSer254 in the function of ETFs.

[1] The abbreviations used are: wETF, electron-transfer flavoprotein from methylotrophic bacterium W3A1; FAD, flavin adenine dinucleotide; TMADH, trimethylamine dehydrogenase; OX, SQ and HQ, the oxidized, semiquinone and hydroquinone states of the flavin cofactor(s), respectively.

In this study, the strength of the hydrogen-bonding interaction at the N(5) of the FAD cofactor in wETF was systematically altered by the substitution of αSer254 with threonine, cysteine, and alanine, which, in principle, should sequentially reduce the H-bond donating strength at this position. The redox potentials and other biochemical properties of αSer254 mutants were analyzed and compared.

MATERIALS AND METHODS

Site-Directed Mutagenesis. The genes encoding the large (α) and small (*β*) subunits of wild-type wETF have been previously cloned into the expression vector pKK223-3 and successfully overexpressed in *Escherichia coli* cells (*29*). Purified recombinant wETF displays spectral and biochemical properties that are indistinguishable from the ETF isolated from the methylotrophic bacterium W3A1 (*29*). The megaprimer polymerase chain reaction approach to site-directed mutagenesis (*32*) was used to create the αS254A, αS254C, and αS254T mutants. The sequences of forward and reverse flanking primers were 5′-CGGTAGTCCAGTG-GTTTCTAATGT-3′ and 5′-CCCACACTACCATCGGCGC-TAC-3′, respectively.

The following mutagenic primers were used (mismatched bases are underscored): αS254T, 5′-GCCTGTTTGAC-CCACCTGTCTGGATT-3′; αS254C, 5′-GCCGCATTGAC-CCACCTGTCTGGATT-3′; αS254A, 5′-GCCTGCTTGAC-CCACCTGTCTGGATT-3′.

Protein Sample Preparation. The wild-type wETF and its αS254 mutants were expressed in *E. coli* cells (strain JM105) and purified as described previously (*29*) except that DEAE-Sephacel and Sephacryl S-200-HR resins were used for the ion-exchange and gel filtration chromatographic steps, respectively. Apoprotein was prepared by extensive dialysis of the holoprotein against 50 mM potassium phosphate buffer, pH 7.2, containing 0.3 mM EDTA and 2.0 M KBr, followed by dialysis against the phosphate−EDTA buffer to remove the KBr.

Spectral Analysis. All ultraviolet−visible absorbance spectra were recorded on a Hewlett-Packard 8452A photodiode array spectrophotometer at 25 °C in 50 mM potassium phosphate buffer, pH 7.2. Raman spectra for the bound FAD were obtained by subtraction of the Raman spectrum of apoETF from that of holoETF, both of which were acquired under identical conditions using nonresonance infrared laser excitation at 752 nm as previously described (*33*, *34*).

Anaerobic Reduction with Sodium Dithionite and the Determination of the Midpoint Potential of the ox/sq Couple ($E_{ox/sq}$). The anaerobic reduction of the protein samples by sodium dithionite and the determination of midpoint potentials of the flavin cofactor are described elsewhere (*10*). All the measurements were performed at 25 °C in 50 mM potassium phosphate buffer, pH 7.2, containing 5% glycerol. The system potential was established based on the spectral changes of the indicator dye toluidine blue ($E_m = +27$ mV versus the standard hydrogen electrode at 25 °C and pH 7) (*35*).

Determination of the Dissociation Constant for the FAD Cofactor and Binding Energy Calculations. The dissociation constants (K_d) for the oxidized state of the FAD cofactor were determined by titrating FAD solutions with freshly prepared apoprotein while monitoring the spectral changes

by ultraviolet−visible spectroscopy. The K_d values were determined by nonlinear regression analyses of the plots of those changes as a function of added apoprotein. The equation used for the curve fitting is

$$\Delta A = \frac{M\left(K + F + \frac{CX}{V} - \sqrt{\left(K + F + \frac{CX}{V}\right)^2 - \frac{4FCX}{V}}\right)}{2F} \quad (1)$$

where ΔA is the difference between the absorbance changes at 462 and 486 nm, K is the dissociation constant (K_d), F is the initial free flavin concentration, C is the effective concentration of the apoprotein, X is the volume of the apoprotein added, V is initial volume, and M is the maximum absorbance change achieved at saturation. Values for K, C, and M were determined from the iterative curve fitting procedure. The K_d values for the anionic SQ state of the FAD cofactor, which is unstable free in solution, were calculated from the thermodynamic box linking the midpoint potential for the ox/sq couple of bound and free FAD and the K_d for the oxidized FAD (*36*) with the equation

$$K_d\,(\mathrm{sq}) = K_d\,(\mathrm{ox})\, e^{(-0.0389\Delta E)} \quad (2)$$

where K_d (ox) and K_d (sq) are K_d values for OX and SQ states, respectively, and ΔE is the difference of $E_{ox/sq}$ (in mV) between free and bound flavins.

Determination of Steady-State Kinetic Parameters. The K_m and k_{cat} values for the reduction of wETF by trimethylamine dehydrogenase (TMADH; 2.3 nM) with trimethylamine (0.25 mM) as its substrate were determined as described previous (*29*). The reaction was initiated with the addition of trimethylamine, and the reduction of wETF was monitored continuously at 440 nm at 25 °C in 50 mM potassium phosphate buffer, pH 7.2. The concentration of wETF was varied between 2 and 50 μM. The k_{cat} and K_m values were determined by the nonlinear regression analysis of a plot of the initial reduction velocity as a function of the concentration of added wETF based on the Michaelis−Menten equation.

RESULTS

Ultraviolet−Visible Absorption Spectra of Wild-Type wETF and α*Ser254 Mutants*. The near-ultraviolet−visible absorbance spectra for the αSer254 mutants were similar to those for wild type (Figure 2), suggesting that the overall environment and the solvent exposure (*37*) of the FAD isoalloxazine ring were generally unchanged. Wavelength shifts were not apparent for the αS254T mutant, which represents the most conservative replacement (Figure 2, inset). However, small spectral red shifts of 2−4 nm were observed in both major absorbance peaks for αS254C and αS254A mutants, which may reflect changes in the strengths of the H-bonding interactions with the isoalloxazine ring (*38*, *39*).

Redox Properties of the Wild-Type wETF and α*Ser254 Mutants.* The wild-type wETF displays an unusual kinetic barrier to the formation of the HQ state (*28*). Prolonged anaerobic incubations with excess sodium dithionite or extended photoreductions in the presence of EDTA and 5-deazariboflavin result only in its reduction to the one-electron reduced state (*26*). The complete reduction to the HQ state by electrochemical methods has been reported; however, the process is extremely slow (*28*). Using this approach, the midpoint potential of the sq/hq couple of wETF was estimated to be −195 mV. This is not an exceptionally low value and suggests that the difficulty in the formation of the HQ is not a thermodynamic issue but rather a kinetic phenomenon. It is also plausible that the FAD was released from the protein during these protracted incubations, whereupon it was rapidly reduced. The enzymatic reduction of wETF by catalytic amounts of TMADH proceeds only to the accumulation of the anionic SQ (*25*). However, when forming complex with TMADH, wETF can be fully reduced to the HQ state both chemically and enzymatically (*40*).

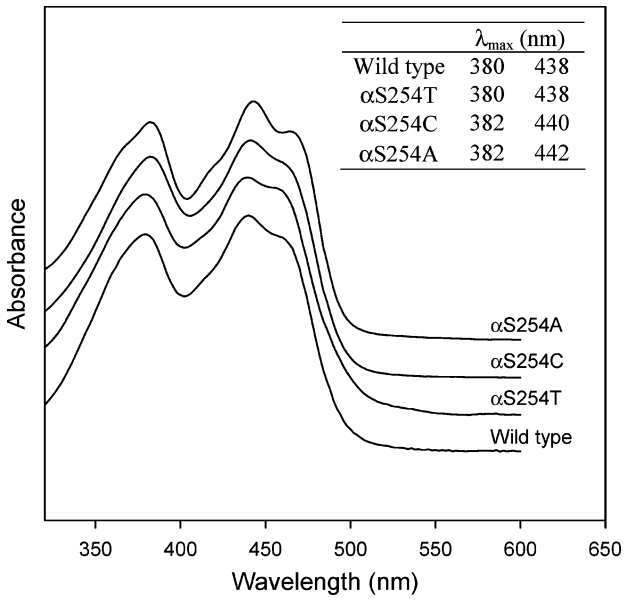

FIGURE 2: Ultraviolet−visible absorption spectra of the wild-type wETF and the αSer254 mutants. The spectra were recorded in 50 mM potassium phosphate buffer, pH 7.2. The spectra are offset for greater clarity. Inset. The λ_{max} values for the two major flavin absorbance peaks.

The results from the reductive titrations of the recombinant wild-type wETF with sodium dithionite were consistent with these reports (Figure 3A). A kinetic barrier was also apparent for the αS254A mutant, with no evidence for the formation of the HQ (Figure 3B), even after several hours of incubation in excess reductant. In marked contrast, the stepwise reduction of the αS254T and αS254C mutants by sodium dithionite proceeded through two well-resolved phases corresponding to the first- and second-electron reductions with the near-stoichiometric accumulation of the anionic SQ at the midway point of the titration (Figure 3C−F). However, the reduction of the anionic SQ to the HQ for both mutants was substantially slower than its formation. The efficient reoxidation of the flavin from the HQ to a stable anionic SQ state with potassium ferricyanide demonstrated that the reduction of each of these two mutants by two electrons was reversible and implies that the formation of HQ state was not due to the release of the flavin.

The midpoint potentials for the ox/sq couple for all of the wETF Ser254 mutants were from 90 to 120 mV lower than that of the wild type (Table 1). The midpoint potential for the αS254T mutant, which represents the most conservative replacement, was the least affected but was still significantly lower than for wild type. The αS254C and αS254A mutants, which should result in either a substantially weaker or the

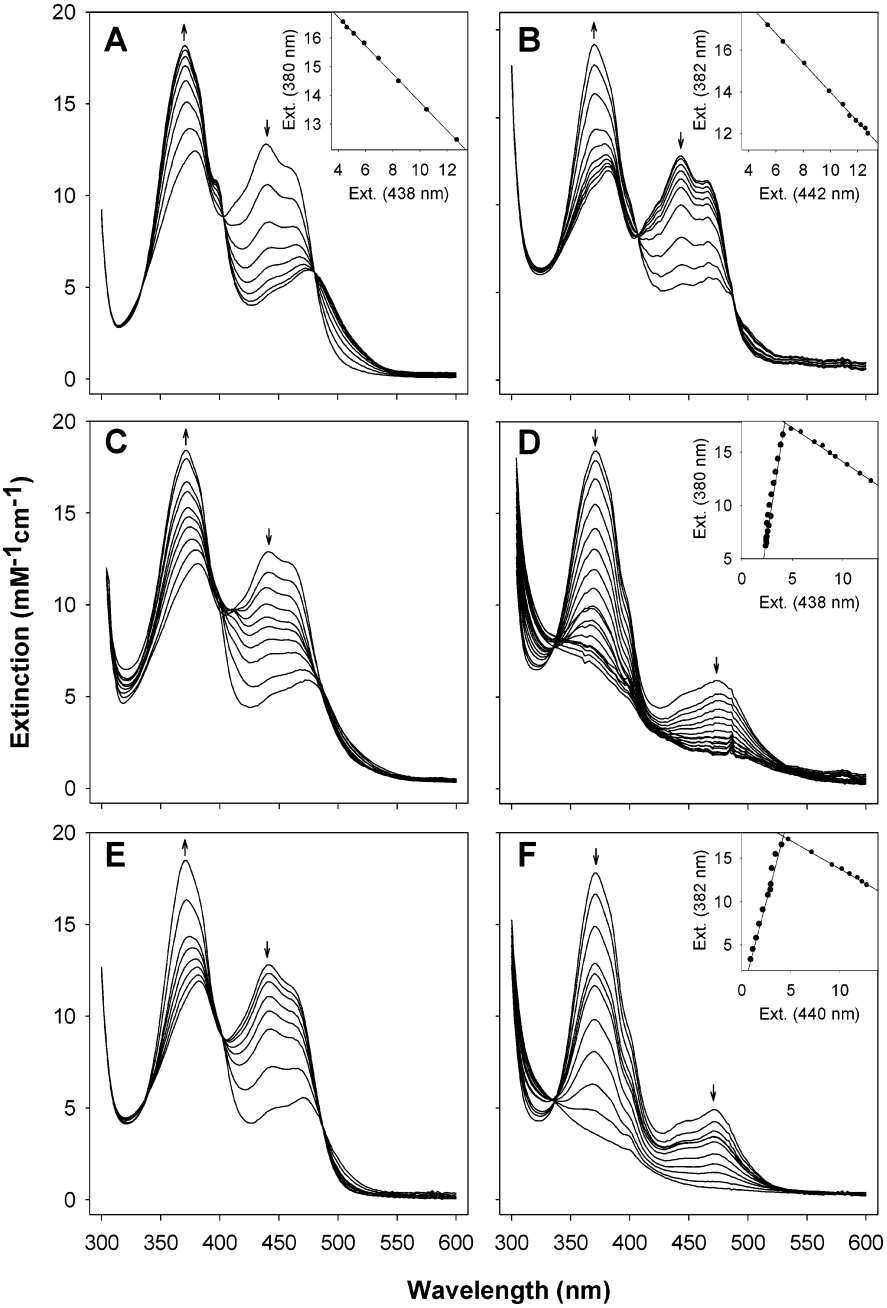

FIGURE 3: Ultraviolet−visible spectral changes induced by the reduction of the wild-type wETF and its αSer254 mutants with sodium dithionite. (A) Wild type; (B) αS254A; (C and D) αS254T; (E and F) αS254C. For wild type and αS254A mutant, reduction proceeded only to the formation of the anionic SQ state even in the presence of excess dithionite and after prolonged incubation times (A and B, respectively). In contrast, the first and second halves (approximate) of the reductive titrations of αS254T (C and D) and αS254C (E and F) to their fully reduced state are shown. The directions of absorbance changes are indicated by the arrows. Inset: Changes in the extinction (Ext) for the two major absorbance peaks during the course of the reductive titrations.

absence of a H-bond with the N(5), exhibited midpoint potentials that were from 15 to 30 mV more negative then for the threonine replacement (Table 1). The midpoint potentials tended to follow the hydrogen-bonding characteristics of the amino acids involved. However, it seems clear that any disruption at this position has a substantial effect on the redox potentials of the FAD cofactor.

Dissociation Constants of FAD for the Wild-Type wETF and aSer254 Mutants. Dissociation constants (K_d) were determined to evaluate the changes in strength of FAD binding to the various αSer254 mutants. The K_d values (Table 1) were observed to increase in the following order: wild type < αS254T < αS254C < αS254A. These results were generally somewhat more consistent with the differences in hydrogen-bond donating strengths of the amino acid replacements. As might be expected, the smallest decrease in binding energy was observed for the αS254T mutant (3.5 kJ/mol) which retains the donor OH group. A larger loss in binding free energy (9.2 kJ/mol) was found for the αS254C mutant, perhaps reflecting the intrinsically weaker H-bonding potential of SH group. However, the loss of binding energy for the αS254A mutant, which cannot participate directly in H-bonding, was similar to the αS254C mutant. These losses are substantially less than the free energy of an average H-bond (~18 kJ/mol) (*2*). However, H-bonding strengths are highly dependent on environment as well as donor and

Table 1: Midpoint Potentials, Dissociation Constants, and Binding Energies for the FAD Cofactor in the Wild-Type wETF and its αSer254 Mutants in the Oxidized and Semiquinone States

		oxidized			semiquinone		
	$E_{ox/sq}$ (mV)	K_d (ox)[a] (nM)	ΔG[b] (kJ/mol)	$\Delta\Delta G$[c] (kJ/mol)	K_d (sq)[d] (pM)	ΔG[b] (kJ/mol)	$\Delta\Delta G$[c] (kJ/mol)
wild type	153 ± 2[e]	12 ± 5	−45	0.0	0.00016	−90	0.0
αS254T	60 ± 5	49 ± 9	−42	3.5	0.024	−78	12
αS254C	32 ± 2	490 ± 10	−36	9.2	0.70	−69	21
αS254A	46 ± 4	590 ± 14	−35	9.7	0.49	−70	20

[a] Determined spectrophotometrically by titration of FAD with apoprotein as described in *Materials and Methods*. [b] Calculated as $\Delta G = 2.4788 \ln K_d$. [c] Change in ΔG relative to wild type. [d] Calculated from the linked equilibria as described in *Materials and Methods* as $K_d(sq) = K_d(ox)e^{(-0.0389\Delta E)}$. [e] From Talfournier et al. (*55*).

acceptor distances and geometry. It is quite plausible that, should space allow, the N(5) of the oxidized FAD could retain a H-bond to a water molecule upon binding. This fixed water molecule could serve as a surrogate donor in the αS254A mutant. Of course, these substitutions could also indirectly affect other interactions involving αSer254 or induce local conformational changes. Nevertheless, the αSer254 replacements were observed to significantly affect flavin binding, and as will be discussed, these effects can be correlated to changes in the interactions with the N(5) atom of the FAD.

Because the midpoint potential for either couple of the flavin cofactor in the flavoproteins is established by the difference in the binding energy between the relevant redox states to the protein (*36*), the K_d values for the wild-type and αSer254 mutants in the SQ state can be calculated from the linked equilibria involving the $E_{ox/sq}$ and the K_d values for the OX state. The K_d values for the anionic SQ increase more dramatically in response to the amino acid substitutions than for the OX state. For example, for the serine to cysteine replacement, the K_d value for the OX state increased ∼40-fold. However, a greater than 4000-fold increase was observed for the SQ state. When translated into Gibbs free energy changes, the replacements resulted in a loss of binding free energy of from 3.5 to 10 kJ/mol for the OX form of the FAD, while the loss of binding energy was at least 2−3-fold greater for the anionic SQ state (Table 1). Thus, the binding of the anionic SQ was more sensitive to the amino acid replacements, and the hydrogen-bonding interactions at the N(5) of the FAD, appear to be more critical for the stabilization of reduced state and, as a result, more responsive to subtle alterations in the strength and configuration of the H-bond as will be discussed below.

Steady-State Kinetic Properties of the Wild-Type wETF and αSer254 Mutants. The steady-state kinetic parameters k_{cat} and K_m for TMADH with the wild-type wETF as the electron acceptor were similar to previously reported values (*41*) and also comparable to those of αS254T mutant (Table 2). However, the values obtained for k_{cat} for the αS254C and αS254A mutants were lower, reflecting impaired electron transfer with TMADH. The K_m values of αS254A mutant are significantly lower than that of the wild type. No obvious correlations are apparent between these steady-state kinetic parameters and the changes in H-bonding on N(5) or the $E_{ox/sq}$ induced by the αSer254 replacements. Based at least on this type of *in vitro* assay, the electron-accepting efficiency of wETF was seemingly unrelated to the presence (as in wild type and the αS254A mutant) or absence (for the αS254T and αS254C mutants) of the kinetic barrier for the formation of the HQ. The absence of such correlations is not surprising because inter-protein electron-transfer mechanisms involve multiple steps, including the formation of the active electron-transfer complex and conformational changes, that can control the transfer rate as discussed further below.

Table 2: Steady-State Kinetic Parameters of Trimethylamine Dehydrogenase with the Wild-Type or αSer254 Mutants of wETF Serving as the Electron Acceptor

	k_{cat} (s^{-1})	K_m (μM)	k_{cat}/K_m ($\mu M^{-1}s^{-1}$)
wild type	13 ± 5	23 ± 7	0.57
αS254T	18 ± 5	21 ± 9	0.86
αS254C	5 ± 2	29 ± 5	0.17
αS254A	1 ± 1	6 ± 3	0.17

Raman Spectra of the Wild-Type wETF and aSer254 Mutants. In the past, we have utilized nuclear magnetic resonance spectroscopy to evaluate the strength and changes of the H-bonding to the N(5) atom of the flavin cofactor in the OX and HQ states in flavodoxin (*4*, *5*). However, this approach was not as readily applicable to the study of the wild-type wETF and its mutants. Therefore, nonresonance Raman spectroscopy was utilized instead. Changes in the Raman spectrum of the FAD cofactor were noted in response to the αSer254 replacements (Figure 4). Raman bands II, III and IV (at approximately 1580, 1550, and 1500 cm^{-1}, respectively) have been assigned to N(5)-relevant vibration modes of the flavin (*33*, *42*−*44*). Changes in the H-bond should alter the electron densities on the bonds at N(5), resulting in frequency shifts for these bands. Such shifts were apparent among this group of proteins. A discernible trend was noted between $E_{ox/sq}$ and the frequencies for all three bands in response to the amino acid replacements, with a lower frequency associated with the lower potentials. This trend is shown in Figure 5 for band III, which has been reported to be insensitive to the conformation of the isoalloxazine ring (*45*) and may be a better marker for changes in the N(5) interactions.

The carbonyl stretching modes for both the C(2)═O and C(4)═O also shifted to lower frequencies in the mutants. Such shifts for the carbonyl band have been linked to stronger hydrogen-bonding interactions on the carbonyl oxygen (*46*), which would imply that the interactions made with both groups are stronger than those in the wild-type protein. But, this may not be the only factor involved. The frequency of the C(4)═O band for the αS254T mutant (1725 cm^{-1}), while lower than for the wild type and the other αSer254 mutants, remains slightly higher than observed in

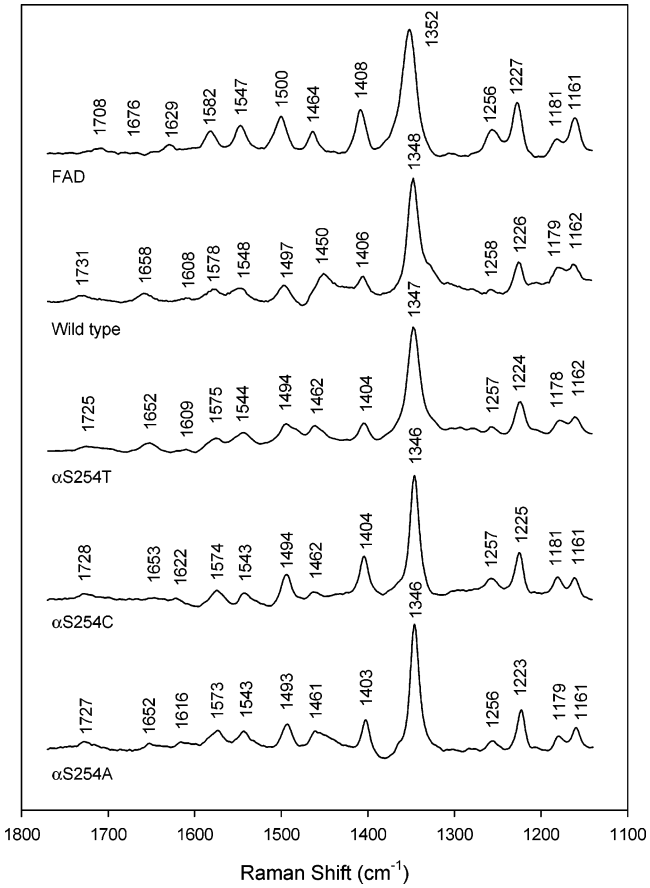

FIGURE 4: Nonresonance Raman spectra of the oxidized states of free FAD, wild-type wETF, and the αSer254 mutants.

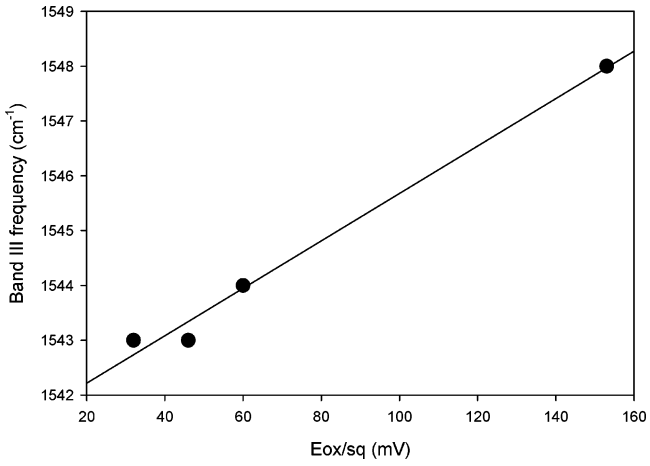

FIGURE 5: Discernible trend between the $E_{ox/sq}$ and the frequency of flavin Raman band III for the wild-type wETF and the three αSer254 mutants.

the riboflavin binding protein (1723 cm^{-1}) (*47*). However, the closest atoms in the binding site of this protein are at least 4.8 Å from the C(4)O, a distance that would seem to preclude the formation of strong hydrogen-bonding interactions (*48*). It is possible, then, that the observed downshifts in the C(4)═O bands in the αSer254 mutants may also be reflecting other slight changes in the local environment that are triggered by alterations involving the polar OH group of αSer254, which is located within 3.3 Å of the C(4)O. Similar indirect structural disturbances may account for the downshifts observed for the C(2)O band in the mutants. For example, the replacements may induce the movement of the αArg237 or other amino acid residues in its immediate vicinity due to the secondary interactions that are made with the side chain OH group of αSer254 (*49*).

Bands I and V, which contain the C−C stretching vibrations from ring I, were also observed to shift to higher frequencies for the αSer254 mutants. These shifts suggest that the environment of the ring I of the FAD is altered by the amino acid replacements as discussed previously (*49*). Unlike the N(5)-relevant bands, the shifts in the carbonyl and ring I bands for the mutants showed low correlations with the changes in $E_{ox/sq}$ and other biochemical properties, which also suggests that they are likely to be the indirect results of the αSer254 substitutions, rather than relevant to the N(5) interaction. As shown in Figure 4, the Raman bands below 1400 cm^{-1} are not sensitive to the αSer254 mutations. The bands between 1100 and 1300 cm^{-1} are derived from the bending vibrations of C(6)−H, C(9)−H, and N(3)−H of the flavin isoalloxazine ring (*33*). These results indicate that the αSer254 mutations have no significant influence on these positions.

DISCUSSION

Effects of the H-Bond on N(5) on the Redox Properties of the Flavin Cofactor in wETF. The N(1) and N(5) loci of the isoalloxazine ring play central roles in establishing the redox properties of the flavin cofactor (*19*, *20*). The chemical characteristics of these two atoms are affected to the greatest extent by the reduction of the flavin and each contributes substantially to the frontier orbitals of the isoalloxazine ring (*20*). Changes in the local environment around these two nitrogen atoms imposed by the binding site within flavoproteins could induce changes in the redox potentials of the flavin and influence the stability of the SQ state (*19*). The effects of the H-bonding interactions on N(1) on the flavin's redox properties have been studied in synthetic model systems and with 4′-deoxy-FAD bound to human ETF (*2*, *3*). The effects of H-bonding at the N(5) of the flavin have also been studied in synthetic model systems in which various protein environments have been simulated (*50*−*53*). The model studies have demonstrated that the H-bond on N(5) plays roles in activating the C(4a) position (*50*), in the stabilization of the anionic SQ form (*51*), and in altering the redox potentials of flavin (*53*). Using flavodoxins as a model flavoprotein system, the role of H-bonding at the N(5)H of the neutral SQ and HQ states of the flavin mononucleotide cofactor has been studied extensively. In these proteins, the carbonyl group of the peptide backbone serves as a H-bond acceptor to the N(5)H of the neutral SQ, an interaction that is crucial for the stabilization of this oxidation state and in the modulation of the midpoint potentials for the first and second couples of the cofactor (*5*, *16*).

Less well understood are the influences of the N(5) interactions in the oxidized and anionic semiquinone states of the flavin cofactor where the N(5) serves as the H-bond acceptor. In this study, this interaction has been investigated in the electron-transfer flavoprotein from the methylotopic bacteria W3A1 in which the side-chain OH group of αSer254 serves as the sole H-bond donor for the N(5). Site-directed replacements of this residue by threonine, cysteine, or alanine were introduced to modulate this interaction by preserving,

weakening, or eliminating this interaction, respectively. The shifts in the N(5)-relevant Raman bands were generally consistent with the intended alterations. Although the threonine side chain retains the OH moiety, the β-methyl group may alter the position of this group relative to N(5) atom, weakening the H-bond on N(5) in the αS254T mutant. The shifts for the αS254C mutant are consistent with the weaker H-bond donating characteristics of the SH group. As observed from the K_d data, the Raman frequency shifts observed for the αS254A mutant are similar to those for the αS254C mutant. Again, the data cannot differentiate between a loss of the H-bonding in the αS254C mutant and perhaps the introduction of a "fixed" water molecule as the H-bond donor in the αS254A mutant. Such surrogate roles for water have been documented for serine to alanine replacements in various proteins.

The H-bond between the N(5) and the side chain of the αSer254 residue of wETF appears to be maintained in the SQ state based on changes in the Raman spectra in response to the replacement of this serine by a cysteine residue (*49*). The K_d values and associated binding free energies (Table 1) also reveal that the amino acid replacements had a greater effect on the anionic SQ state than for the OX state. The H-bonding interaction at N(5) can be rationalized to be stronger in the SQ state due to the greater electron density and the negative charge on the flavin ring compared to the more electron deficient OX state. The stabilization of the neutral flavin SQ by the H-bond on N(5) has been reported in flavodoxins (*5*, *16*) in which the H-bond donor is the N(5)H and the acceptor is a backbone carbonyl oxygen, an interaction promoted by redox-mediated local conformational changes in a flanking loop in the binding site. Alterations in this H-bonding interaction result in changes in $E_{ox/sq}$ that are larger than observed here (*5*, *16*). However, the FAD N(5) in wETF acts as an H-bond acceptor in both the OX and anionic SQ states while in the flavodoxin only the neutral SQ and not the OX form is H-bonded at the N(5). Based on the crystal structures of the OX forms of the human, *Paracoccus denitrificans*, and W3A1 ETF holoproteins, the anionic SQ state is thought to be stabilized by an intraflavin H-bond on N(1), an H-bond between C(2)O and αHis286, and the positive charge from αArg249 (human numbering system) (*27*, *30*, *54*). Because of the negative charge and electron-rich characteristics associated with the isoalloxazine ring of the anionic SQ state, all these interactions are selectively stronger in the anionic SQ state.

Thus, all of the amino acid substitutions introduced in this study were observed to affect the N(5)-related Raman bands and to significantly decrease the midpoint potential of the first couple of the bound FAD in wETF. A trend between the frequency for the N(5)-related Raman band III and the midpoint potential of the first couple in the various wETF variants was apparent (Figure 5). This trend suggests that the frequencies of these Raman bands are all sensitive to changes in the hydrogen-bonding interactions on the N(5). These data, then, provide experimental support for the functional importance of the H-bonding interactions on the N(5) of the FAD cofactor, where N(5) acts as a H-bond acceptor, in establishing the midpoint potential for the first redox couple and the unusual stability of the anionic SQ state in wETF.

Effects of the αSer254 Mutations on the Kinetic Barrier for the sq/hq Couple and Electron-Transfer Activity of wETF. An unusual and fascinating characteristic of the wETF is the kinetic barrier toward the reduction of the anionic SQ to the fully reduced or HQ state, even after prolonged incubations with a strong chemical reductant such as sodium dithionite. The molecular basis of the kinetic barrier is not understood. We initially postulated that the H-bond donating role of αSer254 to the N(5) of the oxidized FAD may assist in the stabilization of the anionic rather than the neutral form of the SQ in this protein. Upon reduction of the flavin, protonation of the N(5) to form the neutral SQ would require that this interaction be broken. This could be avoided by a modest shift of the intrinsic pK_a of 8.3 for the SQ leading to the stabilization of the anionic SQ species. However, the formation of the HQ in wETF would require protonation of the N(5) because of its much higher pK_a value in this redox state and the disruption of the interaction with αSer254. Thus, it was thought that this interaction might interfere with the formation of the HQ state in this protein in this manner. However, we did not observe a good correlation between the alterations of the interactions at N(5) induced by the amino acid replacements and the status of this unusual kinetic barrier. For example, the αS254T and αS254C mutations largely abolished the kinetic barrier. Interestingly, the human ETF, which naturally contains a threonine residue (αThr266) at this position, can also be fully reduced to the HQ state, albeit slowly. More perplexing was the observation that the kinetic barrier was retained in the αS254A mutant. The physical evidence suggested that the strength of the H-bonding interaction with N(5) was comparable in each case. Thus, these results provide an indication that the N(5) interaction alone cannot account for the entire kinetic effect.

The kinetic barrier in wETF has also been reported to be eliminated by the binding of this protein to its redox partner, TMADH, and after substitution of αArg237 by alanine (*40*, *55*). Thus, this behavior may be very complex and could involve multiple residues, conformational changes, or changes in the interactions between domains. Based on the crystal structure of wETF, αArg237 appears to be involved in an interdomain salt bridge with βGlu163 (*27*). This ion pair may help define the rotation angle of the FAD domain relative to the rest of the protein and, thus, may play a central role in the assembly of the electron-transfer complex with TAMDH (*27*). The side chain of αSer254 is located only 3.3 Å away from this glutamate residue. Thus, the threonine and cysteine substitutions for αSer254 may affect the location of the side chain of αArg237 and/or alter its interaction with βGlu163, which then allows for the reduction of the FAD by the second electron. Because the complete lose of the restrictions imposed by the H-bonding interactions in the αS254A mutant, the locations of αAla254 and αArg237 may change significantly, allowing αArg237 to form a new salt bridge, which substantially alters the location of the FAD domain relative to the rest of the protein. This effect may be reflected by the significantly different k_{cat} and K_m values observed for the αS254A mutant (Table 2) due to the importance of domain movement and dynamics during electron transfer (*27*). These effects provide a more plausible explanation for the changes in the kinetic barrier than as a response to the altered midpoint potentials. Therefore, our results provide evidence that αSer254 in wETF not only

modulates the redox potentials of the FAD cofactor but also plays a separate role in the physiological electron-transfer reaction.

Comparing and Contrasting the Redox Properties of wETF and hETF. The wETF shares a similar amino acid sequence and tertiary structure with hETF (*27*, *30*). Although the residues involved in the interactions with the isoalloxazine ring of the FAD are highly conserved among all members of the ETF family, a wide range in the values for $E_{ox/sq}$ is observed (*30*). For instance, the only obvious difference between wETF and hETF is the amino acid residue H-bonded directly to the N(5) of the FAD, being αThr266 in hETF versus αSer254 in wETF (*27*, *30*). Despite this rather conservative difference, the $E_{ox/sq}$ of hETF is ∼130 mV lower than that of wETF (+22 vs +153mV). The replacement of αSer254 in wETF with threonine decreased $E_{ox/sq}$ by 90 mV, but it still remains ∼40 mV higher than that of hETF. Thus, the Ser/Thr interchange could only partially account for much of the difference in $E_{ox/sq}$ between these two ETF proteins. Furthermore, the naturally occurred αT266M variation of the hETF (*31*) and the corresponding αT244M mutation in pETF (*56*) are both reported not to destabilize the SQ state. However, the replacements of αSer254 in wETF significantly destabilize the anionic SQ complex (Table 1). These observations imply that structural factors other than the αSer254/αThr266 interactions, e.g., short-range and long-range electrostatic environments of the flavin cofactor or the different domain conformations of wETF and hEF, could contribute to differences in the midpoint potentials and redox properties of these two proteins. This reminds us that the flavoproteins from a same family, no matter how similar in the amino acid sequence and structure of the flavin binding pocket, may not necessarily share similar redox properties.

REFERENCES

1. Massey, V. (2000) The chemical and biological versatility of riboflavin, *Biochem. Soc. Trans. 28*, 283−96.
2. Dwyer, T. M., Mortl, S., Kemter, K., Bacher, A., Fauq, A., and Frerman, F. E. (1999) The intraflavin hydrogen bond in human electron transfer flavoprotein modulates redox potentials and may participate in electron transfer, *Biochemistry 38*, 9735−45.
3. Guo, F., Chang, B. H., and Rizzo, C. J. (2002) An N1-hydrogen bonding model for flavin coenzyme, *Bioorg. Med. Chem. Lett. 12*, 151−4.
4. Bradley, L. H., and Swenson, R. P. (1999) Role of glutamate-59 hydrogen bonded to N(3)H of the flavin mononucleotide cofactor in the modulation of the redox potentials of the *Clostridium beijerinckii* flavodoxin. Glutamate-59 is not responsible for the pH dependency but contributes to the stabilization of the flavin semiquinone, *Biochemistry 38*, 12377−86.
5. Chang, F. C., and Swenson, R. P. (1999) The midpoint potentials for the oxidized-semiquinone couple for gly57 mutants of the *Clostridium beijerinckii* flavodoxin correlate with changes in the hydrogen-bonding interaction with the proton on N(5) of the reduced flavin mononucleotide cofactor as measured by NMR chemical shift temperature dependencies, *Biochemistry 38*, 7168−76.
6. Hoover, D. M., Drennan, C. L., Metzger, A. L., Osborne, C., Weber, C. H., Pattridge, K. A., and Ludwig, M. L. (1999) Comparisons of wild-type and mutant flavodoxins from Anacystis nidulans. Structural determinants of the redox potentials, *J. Mol. Biol. 294*, 725−43.
7. Ludwig, M. L., Pattridge, K. A., Metzger, A. L., Dixon, M. M., Eren, M., Feng, Y., and Swenson, R. P. (1997) Control of oxidation−reduction potentials in flavodoxin from *Clostridium beijerinckii*: the role of conformation changes, *Biochemistry 36*, 1259−80.
8. Macheroux, P., Kieweg, V., Massey, V., Soderlind, E., Stenberg, K., and Lindqvist, Y. (1993) Role of tyrosine 129 in the active site of spinach glycolate oxidase, *Eur. J. Biochem. 213*, 1047−54.
9. Xu, D., Kohli, R. M., and Massey, V. (1999) The role of threonine 37 in flavin reactivity of the old yellow enzyme, *Proc. Natl. Acad. Sci. U.S.A. 96*, 3556−61.
10. Chang, F. C., and Swenson, R. P. (1997) Regulation of oxidation-reduction potentials through redox-linked ionization in the Y98H mutant of the *Desulfovibrio vulgaris* [Hildenborough] flavodoxin: direct proton nuclear magnetic resonance spectroscopic evidence for the redox-dependent shift in the pK_a of histidine-98, *Biochemistry 36*, 9013−21.
11. Swenson, R. P., and Krey, G. D. (1994) Site-directed mutagenesis of tyrosine-98 in the flavodoxin from *Desulfovibrio vulgaris* (Hildenborough): regulation of oxidation−reduction properties of the bound FMN cofactor by aromatic, solvent, and electrostatic interactions, *Biochemistry 33*, 8505−14.
12. Zhou, Z., and Swenson, R. P. (1995) Electrostatic effects of surface acidic amino acid residues on the oxidation−reduction potentials of the flavodoxin from *Desulfovibrio vulgaris* (Hildenborough), *Biochemistry 34*, 3183−92.
13. Lostao, A., Gomez-Moreno, C., Mayhew, S. G., and Sancho, J. (1997) Differential stabilization of the three FMN redox forms by tyrosine 94 and tryptophan 57 in flavodoxin from Anabaena and its influence on the redox potentials, *Biochemistry 36*, 14334−44.
14. Zhou, Z., and Swenson, R. P. (1996) The cumulative electrostatic effect of aromatic stacking interactions and the negative electrostatic environment of the flavin mononucleotide binding site is a major determinant of the reduction potential for the flavodoxin from *Desulfovibrio vulgaris* [Hildenborough], *Biochemistry 35*, 15980−8.
15. Druhan, L. J., and Swenson, R. P. (1998) Role of methionine 56 in the control of the oxidation−reduction potentials of the *Clostridium beijerinckii* flavodoxin: effects of substitutions by aliphatic amino acids and evidence for a role of sulfur−flavin interactions, *Biochemistry 37*, 9668−78.
16. Kasim, M., and Swenson, R. P. (2000) Conformational energetics of a reverse turn in the *Clostridium beijerinckii* flavodoxin is directly coupled to the modulation of its oxidation−reduction potentials, *Biochemistry 39*, 15322−32.
17. Ludwig, M. L., and Luschinsky, C. L. (1992) Structure and Redox Properties of Clostridial Flavodoxin, in *Chemistry and Biochemistry of Flavoenzymes* (Müller, F., Ed.), pp 427−466, CRC Press, Boca Raton, FL.
18. Watt, W., Tulinsky, A., Swenson, R. P., and Watenpaugh, K. D. (1991) Comparison of the crystal structures of a flavodoxin in its three oxidation states at cryogenic temperatures, *J. Mol. Biol. 218*, 195−208.
19. Massey, V., and Hemmerich, P. (1980) Active-site probes of flavoproteins, *Biochem. Soc. Trans. 8*, 246−57.
20. Hall, L. H., Bowers, M. L., and Durfor, C. N. (1987) Further consideration of flavin coenzyme biochemistry afforded by geometry-optimized molecular orbital calculations, *Biochemistry 26*, 7401−9.
21. Fox, K. M., and Karplus, P. A. (1994) Old yellow enzyme at 2 Å resolution: overall structure, ligand binding, and comparison with related flavoproteins, *Structure 2*, 1089−105.
22. Sevrioukova, I. F., Li, H., Zhang, H., Peterson, J. A., and Poulos, T. L. (1999) Structure of a cytochrome P450-redox partner electron-transfer complex, *Proc. Natl. Acad. Sci. U.S.A. 96*, 1863−8.
23. Abramovitz, A. S., and Massey, V. (1976) Interaction of phenols with old yellow enzyme. Physical evidence for charge-transfer complexes, *J. Biol. Chem. 251*, 5327−36.
24. Kasim, M. (2002) Ph.D. Thesis, The Ohio State University, Columbus, OH.
25. Steenkamp, D. J., and Gallup, M. (1978) The natural flavoprotein electron acceptor of trimethylamine dehydrogenase, *J. Biol. Chem. 253*, 4086−9.
26. Davidson, V. L., Husain, M., and Neher, J. W. (1986) Electron transfer flavoprotein from Methylophilus methylotrophus: properties, comparison with other electron transfer flavoproteins, and regulation of expression by carbon source, *J. Bacteriol. 166*, 812−7.
27. Leys, D., Basran, J., Talfournier, F., Sutcliffe, M. J., and Scrutton, N. S. (2003) Extensive conformational sampling in a ternary electron transfer complex, *Nat. Struct. Biol. 10*, 219−25.

28. Byron, C. M., Stankovich, M. T., Husain, M., and Davidson, V. L. (1989) Unusual redox properties of electron-transfer flavoprotein from *Methylophilus methylotrophus*, *Biochemistry 28*, 8582−7.
29. Chen, D., and Swenson, R. P. (1994) Cloning, sequence analysis, and expression of the genes encoding the two subunits of the methylotrophic bacterium W3A1 electron transfer flavoprotein, *J. Biol. Chem. 269*, 32120−30.
30. Roberts, D. L., Frerman, F. E., and Kim, J. J. (1996) Three-dimensional structure of human electron transfer flavoprotein to 2.1-Å resolution, *Proc. Natl. Acad. Sci. U.S.A. 93*, 14355−60.
31. Salazar, D., Zhang, L., deGala, G. D., and Frerman, F. E. (1997) Expression and characterization of two pathogenic mutations in human electron transfer flavoprotein, *J. Biol. Chem. 272*, 26425−33.
32. Barik, S. (2002) Megaprimer PCR, *Methods Mol. Biol. 192*, 189−96.
33. Zheng, Y., Dong, J., Palfey, B. A., and Carey, P. R. (1999) Using Raman spectroscopy to monitor the solvent-exposed and "buried" forms of flavin in *p*-hydroxybenzoate hydroxylase, *Biochemistry 38*, 16727−32.
34. Altose, M. D., Zheng, Y., Dong, J., Palfey, B. A., and Carey, P. R. (2001) Comparing protein-ligand interactions in solution and single crystals by Raman spectroscopy, *Proc. Natl. Acad. Sci. U.S.A. 98*, 3006−11.
35. Clark, W. M. (1972) *Oxidation-reduction potentials of organic systems*, Robert E. Krieger Publishing Co., Huntington, NY.
36. Dubourdieu, M., le Gall, J., and Favaudon, V. (1975) Physicochemical properties of flavodoxin from Desulfovibrio vulgaris, *Biochim. Biophys. Acta 376*, 519−32.
37. Eweg, J. K., and Mueller, F. (1980) Helium (HeI) and (HeII) photoelectron spectra of alloxazines and isoalloxazines, *J. Am. Chem. Soc. 102*, 51−61.
38. Nishimoto, K., Watanabe, Y., and Yagi, K. (1978) Hydrogen bonding of flavoprotein. I. Effect of hydrogen bonding on electronic spectra of flavoprotein. *Biochim. Biophys. Acta 526*, 34−41.
39. Yagi, K., Ohishi, N., Nishimoto, K., Choi, J. D., and Song, P. S. (1980) Effect of hydrogen bonding on electronic spectra and reactivity of flavins, *Biochemistry 19*, 1553−7.
40. Jang, M. H., Scrutton, N. S., and Hille, R. (2000) Formation of W(3)A(1) electron-transferring flavoprotein (ETF) hydroquinone in the trimethylamine dehydrogenase · ETF protein complex, *J. Biol. Chem. 275*, 12546−52.
41. Wilson, E. K., Huang, L., Sutcliffe, M. J., Mathews, F. S., Hille, R., and Scrutton, N. S. (1997) An exposed tyrosine on the surface of trimethylamine dehydrogenase facilitates electron transfer to electron transferring flavoprotein: kinetics of transfer in wild-type and mutant complexes, *Biochemistry 36*, 41−8.
42. Lively, C. R., and McFarland, J. T. (1990) Assignment and the effect of hydrogen bonding on the vibrational normal modes of flavins and flavoproteins, *J. Phys. Chem. 94*, 3980−94.
43. Wille, G., Ritter, M., Friedemann, R., Mantele, W., and Hubner, G. (2003) Redox-triggered FTIR difference spectra of FAD in aqueous solution and bound to flavoproteins, *Biochemistry 42*, 14814−21.
44. Unno, M., Sano, R., Masuda, S., Ono, T., and Yamauchi, S. (2005) Light-Induced Structural Changes in the Active Site of the BLUF Domain in AppA by Raman Spectroscopy, *J. Phys. Chem. B 109*, 12620−12626.
45. Tegoni, M., Gervais, M., and Desbois, A. (1997) Resonance Raman study on the oxidized and anionic semiquinone forms of flavocytochrome b2 and L-lactate monooxygenase. Influence of the structure and environment of the isoalloxazine ring on the flavin function, *Biochemistry 36*, 8932−46.
46. Hazekawa, I., Nishina, Y., Sato, K., Shichiri, M., Miura, R., and Shiga, K. (1997) A Raman study on the C(4)=O stretching mode of flavins in flavoenzymes: hydrogen bonding at the C(4)=O moiety, *J. Biochem. (Tokyo) 121*, 1147−54.
47. Kim, J. J., Wang, M., and Paschke, R. (1993) Crystal structures of medium-chain acyl-CoA dehydrogenase from pig liver mitochondria with and without substrate, *Proc. Natl. Acad. Sci. U.S.A. 90*, 7523−7.
48. Monaco, H. L. (1997) Crystal structure of chicken riboflavin-binding protein, *Embo. J. 16*, 1475−83.
49. Yang, K.-Y., and Swenson, R. P. (2007) Non-resonance Raman study of the flavin cofactor and its interactions in the methylotrophic bacterium W3A1 electron transfer flavoprotein. *Biochemistry, 46*, 2298−2305.
50. Shinkai, S., Honda, N., Ishikawa, Y., and Manabe, O. (1985) Coenzyme models. 41. On the unusual reactivities of N(5)-hydrogen-bonded flavin. An approach to regiospecific flavin activation through hydrogen bonding, *J. Am. Chem. Soc. 107*, 6286−92.
51. Akiyama, T., Simeno, F., Murakami, M., and Yoneda, F. (1992) Flavin-6-carboxylic acids as novel and simple flavoenzyme models. Nonenzymatic stabilization of the flavin semiquinone radical and the 4a-hydroperoxyflavin by intramolecular hydrogen bonding, *J. Am. Chem. Soc. 114*, 6613−20.
52. Breinlinger, E., Niemz, A., and Rotello, V. M. (1995) Model Systems for Flavoenzyme Activity. Stabilization of the Flavin Radical Anion through Specific Hydrogen Bond Interactions, *J. Am. Chem. Soc. 117*, 5379−80.
53. Kajiki, T., Moriya, H., Kondo, S., Nabeshima, T., and Yano, Y. (1998) Remarkable stabilization of the anionic semiquinone radical of 6-azaflavin by hydrogen bonding with a receptor in chloroform, *Chem. Commun. 24*, 2727−8.
54. Roberts, D. L., Salazar, D., Fulmer, J. P., Frerman, F. E., and Kim, J. J. (1999) Crystal structure of *Paracoccus denitrificans* electron transfer flavoprotein: structural and electrostatic analysis of a conserved flavin binding domain, *Biochemistry 38*, 1977−89.
55. Talfournier, F., Munro, A. W., Basran, J., Sutcliffe, M. J., Daff, S., Chapman, S. K., and Scrutton, N. S. (2001) alpha Arg-237 in Methylophilus methylotrophus (sp. W3A1) electron-transferring flavoprotein affords approximately 200-millivolt stabilization of the FAD anionic semiquinone and a kinetic block on full reduction to the dihydroquinone, *J. Biol. Chem. 276*, 20190−6.
56. Griffin, K. J., Dwyer, T. M., Manning, M. C., Meyer, J. D., Carpenter, J. F., and Frerman, F. E. (1997) alphaT244M mutation affects the redox, kinetic, and in vitro folding properties of *Paracoccus denitrificans* electron transfer flavoprotein, *Biochemistry 36*, 4194−202.

BI0616293